

COMPARATIVE ANALYSIS OF STRUCTURE FORMATION AND PROPERTIES OF PVD COATINGS TIN, TI/TIN AND TIN-MON

Nataliia Pinchuk¹

DOI: <https://doi.org/10.30525/978-9934-26-297-5-19>

Abstract. Nanocomposite coatings represent a new generation of materials and they consist of at least two phases with a nanocrystalline and/or amorphous structure. They have a lot of unique properties, the appearance of which is associated with a high volume fraction of phase boundaries, with the strength of these boundaries, with the absence of dislocations inside crystals. *The purpose* of the paper analysis of the reasons for the observed changes, based on the mechanism of formation of surface layers of vacuum-arc coatings under the condition of implantation processes stimulated by applying a negative potential to the substrate. *Methodology.* All samples were obtained using modern coating methods on a modernized "Bulat-6" installation. Cross section images were carried out by methods of optical, electron microscopy. Structure of the samples was studied using a "DRON-3M" instrument in Cu-K α radiation. Separation of diffraction profiles was carried out using the "New profile". Mechanical tests of materials were performed in the mode of microindentation. *Results.* At all schemes of deposition of TiN coatings, a single-phase state with an fcc lattice is formed. As the displacement potential increases, a transition from [100] to [111] texture is observed. In multilayer nanostructured TiN/Ti coatings, a texture develops in titanium nitride layers with a thickness of 300 nm or more when a displacement potential is applied [111]. The thickness of the Ti layers of more than 30 nm is sufficient for the development of the stress-strain state in the TiN layers without their significant relaxation. When the displacement potential increases, the macrostress of the compression in the titanium nitride layers of TiN increases. It was established that epitaxial growth of isostructural cubic modifications of titanium nitride and molyb-

¹ Candidate of Physical and Mathematical Sciences (PhD),
Researcher, Department of Materials Science,
National Technical University "Kharkiv Polytechnic Institute", Ukraine;
Visiting researcher, Department of Engineering and Physics,
Karlstad University, Sweden

denum nitride without the formation of a two-phase state is possible with a small thickness of layers in the TiN-Mo₂N multilayer system (≈ 2 nm). At a greater thickness, a two-phase material is formed, where the second phase is high-temperature molybdenum nitride γ -Mo₂N with a cubic lattice, which is isostructural to titanium nitride. *Practical implications.* The final properties of nanocrystalline coatings such as the size and orientation of the grains, the structure strongly depend on the technological parameters of deposition – ion bombardment, shear potential, temperature of the substrate, flow density and energy of the precipitating ions, therefore, in order to achieve the desired results in each specific case, it is necessary to strive for optimization of the process deposition of coatings. *Value/originality.* A possible mechanism for the formation of micro- and nanostructured layered condensates under conditions of continuous influence of condensation of accelerated particles of the deposited flow is proposed. At the same time, the surface is subject to bombardment, which is based on radiation-stimulated processes of redistribution of elements of the deposited flow and structural defects of the coating material that is formed.

1. Introduction

Vacuum-arc deposition of coatings for various purposes has become widespread in the last few decades. The unique capabilities of the method are due to the specifics of the vacuum arc used in it as the main technological tool. Among various ion-plasma techniques, vacuum-arc is one of the most versatile due to the high degree of ionization of the flow of film-forming particles and good adhesion properties of coatings to substrates.

At this time, great attention is paid to obtaining and researching the properties of submicron, nanocrystalline materials due to their application in various fields of technology, such as electronics, catalysis, magnetic data storage, structural components, etc. [1–3].

Technological possibilities of the vacuum-arc method: bombarding the growing surface with energetic ions allows influencing the size of structural elements in the process of forming coatings, and on the other hand, controlling the size and orientation of grains, structure, possibly by doping, adding one or more elements to the main coating material, thus preventing the growth of grains of the main phase, which leads to dimensional effects of thermodynamic quantities.

The analysis of literature data shows that even quite thin wear-resistant coatings wear off quickly. The physics of the strength of crystalline bodies, based on dislocation representations, gives recommendations for obtaining a massive high-strength coating in the form of a sandwich, in which thin layers of one phase compound must be interspersed with equally thin layers of another compound. Therefore, the study of patterns of formation of layered nanostructured films based on nitrides and carbides of refractory materials (Ti, Zr, Mo, Cr, Ti, Al, Nb, Hf) is of practical and scientific interest.

2. Methodology of obtaining and researching single-layer and multi-layer vacuum-arc coatings

The coatings were obtained in the Bulat-6 vacuum-arc installation. The block diagram of the installation is shown in Figure 1. Vacuum chamber 1 is equipped with a system of automatic maintenance of nitrogen pressure 2 and two evaporators, one of which 3 contains high-purity molybdenum that was remelted in a vacuum as the evaporated material, and the other 4 – titanium of the VT1-0. A substrate holder 5 in the form of a stainless steel plate measuring 300x300 mm is installed on the rotating device of the camera, in the center of which there are substrates 6. Polished substrates made of stainless steel 12Cr18Ni9Ti (AISI 321) with dimensions of 20×20×3 mm and copper foil with a thickness of 0.2 mm were used as the basis, which were previously washed with an alkaline solution in an ultrasonic bath and then with nefras C2-80/120. The installation is also equipped with a constant voltage source 7, the value of which can be changed within 5...1000 V, as well as a pulse voltage generator 8 with an adjustable pulse amplitude within 0.5...2 kV and a compliance frequency of 0.5...7 kHz.

The rotary device is electrically isolated from the vacuum chamber and withstands voltages over 3 kV. Its mechanism provides a rotation speed of 8 rpm. The chamber is equipped with an extraction unit with steam-oil and mechanical vacuum pumps.

After pumping out the vacuum chamber to a pressure of $p_{N_2} = 2.7 \cdot 10^{-3}$ Pa, a negative potential of 1000 V was applied to the substrates, and at an arc current $I_d = 90$ A, their surface was cleaned and activated by bombardment with titanium ions for 3 ÷ 4 min. Then deposition of titanium layers was carried out at residual gas pressure $p_{N_2} = 2.7 \cdot 10^{-3}$ Pa and TiN layers at a nitrogen pressure of $p_{N_2} = 6.7 \cdot 10^{-1}$ Pa. The average application speed was

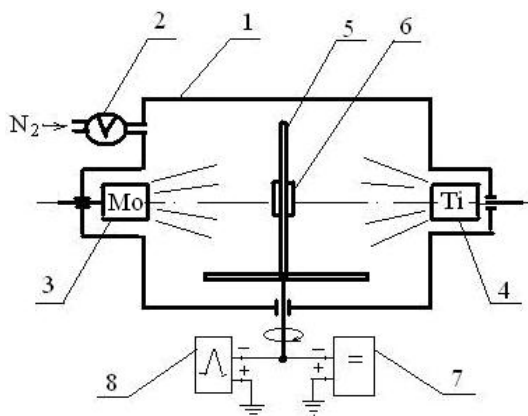


Figure 1. Scheme of the installation for applying multilayer coatings:
1 – vacuum chamber; 2 – system of automatic maintenance of nitrogen pressure; 3 – molybdenum evaporator;
4 – titanium evaporator; 5 – substrate holder; 6 – substrate;
7 – source of constant voltage; 8 – pulse voltage generator

1nm/s. The number of layers with different thicknesses was selected in such a way that the total thickness of the coating was about 7 microns. The value of the substrate's negative potential (U_p) varied from the "floating" potential (it was set self-consistently and was $-3 \dots -15$ V), -40 V, -70 V, -200 V. The modes of obtaining coatings are listed in Table 1.

The process of deposition of TiN-MoN multilayer coatings was carried out under the following technological conditions. After the deposition of the first layer (in this case, 10 s or 20 s), both evaporators were turned off, the substrate holder was turned 180°C , and both evaporators were simultaneously turned on again. Thus, layers were deposited for 10 s and 20 s on a stationary substrate. The layer was deposited for 3 s on a rotating substrate (12 rpm). In front of each evaporator, the substrate was exposed for 3 s, rotating at the same time by 180°C . At an average deposition rate of about 1 nm/s, this mode corresponded to a thickness of one layer of about 2 nm. The arc current in the deposition process was 85...90 A, the nitrogen pressure in the chamber was $6.7 \cdot 10^{-1}$ Pa, the distance from the evaporator to the substrate was 250 mm, the temperature of the substrate was in the range

Table 1

Modes of obtaining vacuum-arc coatings of the single-layer TiN and multilayer Ti/TiN system

Sample №	I_d , A	U_p , V	p_N , Pa / (time of deposition)	Number of two-layer periods
Single-layer TiN				
S1	90	-3...-5	$6.7 \cdot 10^{-1}$ Pa (1.5 h)	-
S2	90	-200	$6.7 \cdot 10^{-1}$ Pa (1.5 h)	-
Multilayer Ti/TiN system				
M1	90	-200	$2.7 \cdot 10^{-3}$ Pa (30 sec) / $6.7 \cdot 10^{-1}$ Pa (300 sec)	20
M2	90	-70	$2.7 \cdot 10^{-3}$ Pa (30 sec) / $6.7 \cdot 10^{-1}$ Pa (300 sec)	20
M3	90	-40	$2.7 \cdot 10^{-3}$ Pa (30 sec) / $6.7 \cdot 10^{-1}$ Pa (300 sec)	20
M4	90	-3...-5	$2.7 \cdot 10^{-3}$ Pa (30 sec) / $6.7 \cdot 10^{-1}$ Pa (300 sec)	20
M5	85	-200	$2.7 \cdot 10^{-3}$ Pa (120 sec) / $6.7 \cdot 10^{-1}$ Pa (780 sec)	8
M6	85	-200	$2.7 \cdot 10^{-3}$ Pa (240 sec) / $6.7 \cdot 10^{-1}$ Pa (780 sec)	7
M7	85	-200	$2.7 \cdot 10^{-3}$ Pa (120 sec) / $6.7 \cdot 10^{-1}$ Pa (120 sec)	30

of 250...350 °C. At a deposition time of 10 s and 20 seconds, one pair of two TiN-MoN nanolayers had a thickness of about 20 nm or 40 nm, while the thickness of each nanolayer was about 10 nm or 20 nm, respectively. In the process of deposition of coatings, pulses of negative potential with a duration of 10 μ s with a frequency of 7 kHz and an amplitude of 2 kV were applied to the substrate, as well as a constant negative potential of 5...400 V. Annealing of samples with coatings was done in a vacuum furnace at a residual gas pressure of $1.3 \cdot 10^{-3}$ Pa and temperature of 800°C for 2 h after reaching this temperature.

X-ray diffraction structural studies of the samples were carried out on a DRON-3 diffractometer in Cu-K α radiation while recording scattering in the discrete shooting. The exposure time per dot was 20...100 s. Separation of diffraction profiles in the case of their superimposition was carried out using the "New profile" line separation program developed by NTU "KhPI", which are superimposed. The volume fraction of phases in the film was calculated according to the standard method, which takes into account the integral intensity and reflectivity of several lines of each of the phases. Analysis of the phase composition was carried out using the ASTM file.

The method of constructing "*a-sin2ψ-graphs*" was used to determine the stress state. The "*a-sin2ψ*" method and its modification (the "crystal group" method [4–5]) were used to study the macrostrain state with a pronounced texture. It is based on the fact that in the presence of macrostresses, each element of the sample is generally subject to the action of three main stresses σ_1 , σ_2 , σ_3 . In addition to texture planes, reflections from planes (420), (422) and (511) at angles ψ corresponding to texture planes were used as the basis for determining elastic microdeformation.

Processing of the received diffraction profiles was carried out on a computer using the Origin 7.5 and NewProfile 3.4 programs. This software allows you to quickly construct diffraction curves from the obtained data array, perform initial processing of the profile and decompose the complex profile into components, which is necessary for the calculation of the sub-structural characteristics of the sample.

3. Vacuum arc coatings TiN

Technological parameters of deposition are of great importance for the formation of coatings. Therefore, such important parameters were chosen as the main structure-forming parameters in the work, such as: the pressure of the working nitrogen atmosphere during application; constant negative bias potential applied to the substrate during the deposition process.

It should also be noted that today the most promising are multilayer coatings with a nanoscale period, which provide a set of unique properties, namely: high wear resistance, corrosion resistance, superhardness, low friction coefficient, etc. Based on this, there is an increasing interest in the features of the formation of multilayer coatings with different combinations of elements depending on the deposition conditions. Therefore, the next stage of the work will be the study of the features of the formation of multilayer Ti/TiN vacuum-arc coatings.

On Figure 2 show fractograms of coating fractures obtained at pressures of $6.7 \cdot 10^{-1}$ Pa. It can be seen that at this only traces of drops are visible in the coatings and this coating has a columnar structure. This is due to a more intense atomization of the droplet phase due to an increase in the number of nitrogen atoms in the working space of the chamber.

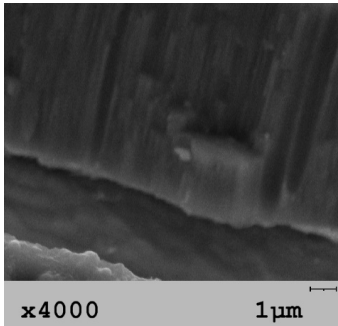


Figure 2. Fracture of single-layer TiN coating (S2) on a copper substrate obtained at $U_p = -200$ V (8 μm thick)

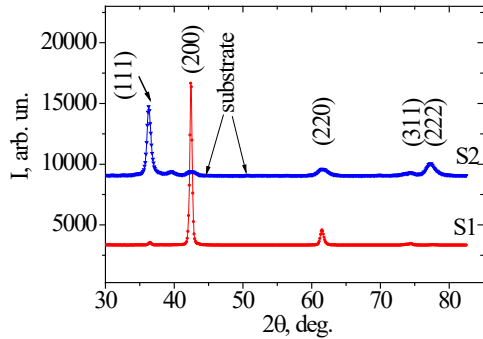


Figure 3. X-ray diffraction spectra from TiN coatings obtained at $p_N = 6.7 \cdot 10^{-1}$ Pa: S1 – $U_p = (-5 \dots -8)$ V; S2 – $U_p = -200$ V

The results of a comparison of X-ray structural analysis of TiN coatings obtained at a "floating" constant potential, as well as $U_p = -200$ V, at a nitrogen atmosphere pressure of $6.7 \cdot 10^{-1}$ Pa are shown in Figure 3.

At the same time, the formation of TiN coatings with a clearly expressed axis of the predominant crystallite orientation [100] occurs (Figure 3, spectrum S1). In the case of supplying a large $U_p = -200$ V (Figure 3, spectrum S2), the predominant orientation with the axis of the texture is formed [111].

The study of substructural characteristics was carried out by the method of approximation of the shape of diffraction reflexes from two orders of reflection. For coatings obtained at $p_N = 6.7 \cdot 10^{-1}$ Pa and a "floating" constant potential, the size of the crystallites (L) decreased to 24 nm, and the microdeformation ($\langle \epsilon \rangle$) was equal to 0.12%. Applying a large constant potential of -200 V leads to an increase in L from 53 nm to 91 nm and a noticeable increase in $\langle \epsilon \rangle$ from 0.37% to 0.7%.

As is known, one of the critical parameters that determine the physical and mechanical properties of coatings and their further performance is macrostrain [6]. In the coatings obtained at $p_N = 6.7 \cdot 10^{-1}$ Pa, the amount of macrodeformations was about -0.1% for the "floating" potential and -1.95% for $U_p = -200$ V. The hardness of these coatings was almost the same and reached the value of 26-28 GPa.

The main characteristics of the impact on the formation of titanium nitride were analyzed. The next stage of research is multilayer coatings based on TiN.

4. Multilayer coatings Ti/TiN

The interest in nanolayered structures such as ceramic superlattices is connected with the fact that the materials created on their basis have very high strength, stiffness and hardness [7; 8]. Systems of several layers of nitrides are superior in hardness to the corresponding monolithic phases, which led to interest in research and the possibility of applying nitride multilayer coatings. It should be noted that multilayer structures, despite the complexity of their manufacture, can be considered as systems for the transition to even more complex systems obtained by deposition methods. The study of multilayer coatings should become the next stage in the theoretical and practical research of nanotechnology materials of the future. In addition, multilayer coatings can serve as a very useful model for studying the properties of materials with so-called reduced or fractional dimensionality, which is very important for studying the mechanical characteristics of complex nanocomposites. And in this connection, it is possible to note a good prospect for the use of transition metal/transition metal nitride systems, the most interesting of which is the Ti/TiN system.

On Figure 4 a, b are photographs of a typical structure of multilayer coatings with relatively thin (125 nm) and thick (600 nm) TiN layers. It can be seen that the columnar grain growth structure characteristic of a single-layer thick TiN coating (Figure 1, with a thickness close to the total thickness of the multilayer condensate (7–8 μm) for comparison with multilayer coatings) is also traced in relatively thick TiN layers of a multilayer coating (Figure 4 a).

It is also possible to note a rather high planarity of the interlayer boundary, both at a relatively small (about 125 nm) and at a relatively large (about 780 nm) thickness of the TiN layer (Figure 4 b, a).

For multilayer coatings, the two-phase nature also show in X-ray spectra, in which diffraction peaks were observed from titanium nitride TiN (cubic crystal lattice of the NaCl structural type) and α -Ti phase. Figure 5 shows the diffraction spectra of samples obtained at different substrate potentials U_p and deposition time of 30 s at a nitrogen gas pressure of $2.7 \cdot 10^{-3}$ Pa. (i.e.

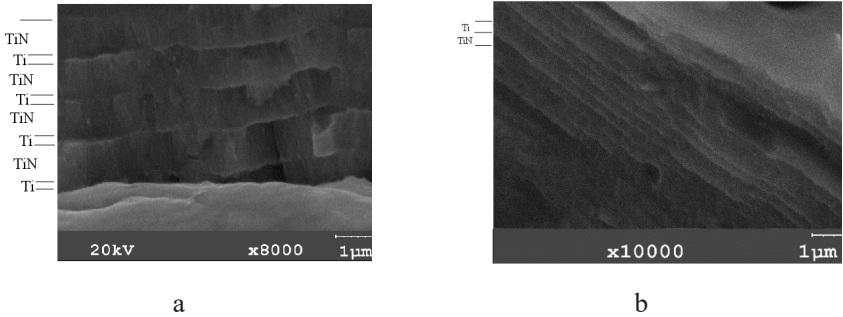


Figure 4. Fracture of multilayer and Ti/TiN coatings (on a copper substrate obtained at $U_p = -200$ V: a, b – samples M6 and M7, respectively

when practically pure titanium is deposited) and 300 s at a nitrogen atmosphere pressure of $6.7 \cdot 10^{-1}$ Pa, at which titanium nitride is formed.

With an increase in U_p , the intensity of the α -Ti diffraction peaks decreases, which may be due to a wider near-boundary mixing with the formation of titanium nitride in the near-boundary region. Titanium nitride TiN

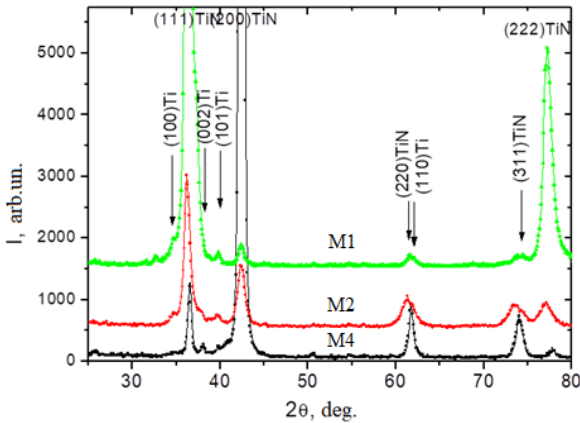


Figure 5. Sections of diffraction spectra from multilayer coatings of the TiN (300 nm)/Ti (30 nm) system, obtained at substrate potentials: M4 – $U_p = -(3 \div 15)$ V; M2 – $U_p = -70$ V; M1 – $U_p = -200$ V

is characterized by a predominant orientation of crystallites, which changes from [100] at a potential on the substrate close to zero ("floating") to [111] at high negative bias potentials.

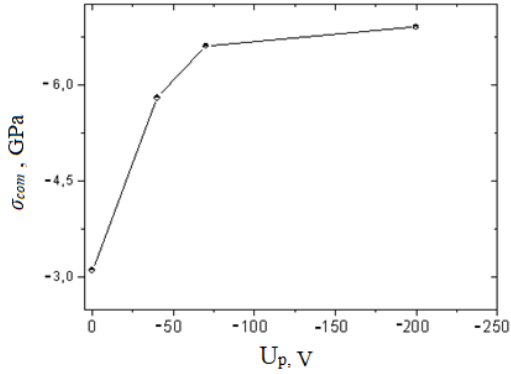
The elastically stressed state of the coatings was determined by the method of multiple oblique surveys (" $a\text{-sin}2\psi$ "-method). An analysis of the stress state in the layers of titanium nitride TiN by the slope of the " $a\text{-sin}2\psi$ " graphs indicates the compressive nature of the stresses developing in the coating. On Figure 6 shows the dependences of the stress state in layers of titanium nitride TiN about 300 nm thick, and the period of the crystal lattice of TiN in the unstressed section of the " $a\text{-sin}2\psi$ " graph (for $a\text{-sin}2\psi_0 = 2\nu/(1+\nu)$, where ν is Poisson's ratio) on the negative bias potential on the substrate. It can be seen (Figure 6 a) that a strong dependence $\sigma_{com}(U_p)$ is observed up to $U_p = -70$ V. At a higher bias potential, the compression stresses change slightly, approaching the value $\sigma_{com} = -7$ GPa.

The dependence of the lattice period on the bias potential has a non-monotonic character: a sharp increase in a at small U_p with a further slight decrease (Figure 6 b).

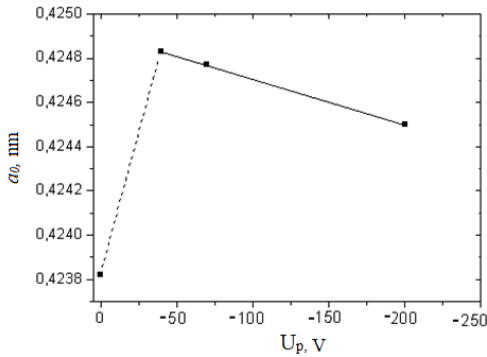
In the final part of the study of the structurally deformed state, a comparison of the structure and the stress state of the TiN/Ti system with different thickness (size factor) of the Ti layer was carried out.

From Figure 7 it can be seen that even with the smallest thickness of the TiN layer (125 nm, sample M7), a texture with a (111) plane parallel to the growth surface is formed, but its degree of perfection is not high. In titanium layers with a hexagonal lattice, a texture with a base plane (001) parallel to the growth surface is formed. The formation of such a texture in the hexagonal titanium crystal lattice can be determined by the position of titanium atoms in the (111) plane of the fcc lattice of TiN layers.

In this case, the titanium hexagonal lattice period $a = 0.29586$ nm, which is close to the tabular value, and the titanium lattice period $c = 0.47249$ nm, which slightly exceeds the tabular values. The increased lattice period c , according to [9], indicates the presence of interstitial atoms, such as nitrogen, in the interstices. With a thinner titanium layer (30 nm), both the lattice period $a = 0.29601$ nm and the period $c = 0.48344$ nm are increased, which indicates a very high content of impurity (nitrogen) atoms in this layer and the development of compressive stresses.



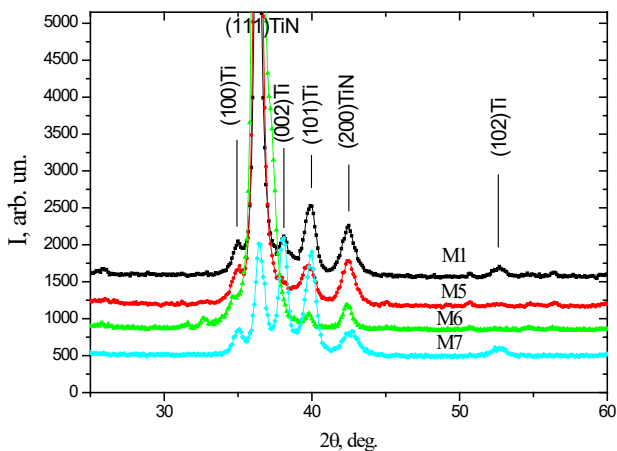
a



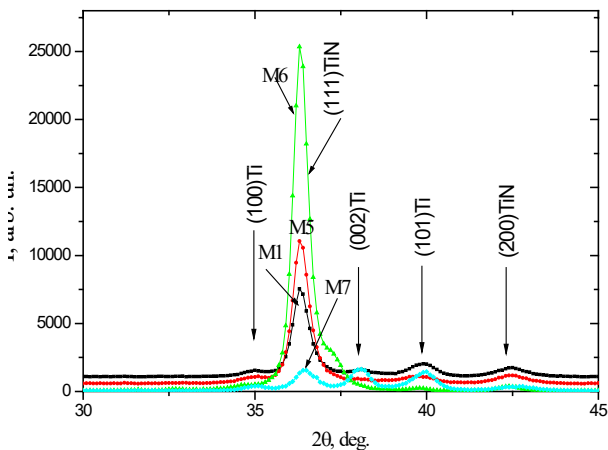
b

Figure 6. Dependence of the compression stress σ_{com} (a) and the lattice period a_0 in the unstressed section (b) on the substrate potential U_p for the TiN(300 nm)/Ti(30 nm) multilayer system (samples M4, M3, M2, M1)

It should be noted that at a relatively high volume content of Ti (about 50%) in the M7 multilayer coating, a relatively low degree of texturization of TiN crystallites with the (111) plane parallel to the growth surface is observed. With an increase in the thickness of the TiN layer to 300 nm and a low volume content of Ti (10%) or with a thicker TiN layer (780 nm) and a high volume content of Ti (20 and 30%), the (111) TiN texture



a



b

Figure 7. Sections of diffraction spectra from a multilayer TiN/Ti system with different layer thicknesses obtained at $U_p = -200$ V (samples M1, M5, M6, M7): a – general view of the spectrum section, b – region of the most intense reflections

becomes stronger. The degree of texture, which is the ratio of the integral intensities of the peaks from the (111) and (200) planes, increases from $I(111)/I(200) = 4.1$ for the M7 multilayer coating to 10.7; 18.7 and 59 for coatings M1, M5 and M6, respectively.

The data of X-ray tensometry (" $a\text{-sin}2\psi$ "-method) showed that with the smallest thickness of the TiN layer equal to 125 nm (the specific volume in the multilayer coating is about 50%, which is equivalent to a thickness of 3.5 μm of the TiN layer), the compression stresses at $U_p = -200$ V are -5.5 GPa. This is somewhat less than in thicker layers (300 nm). Thus, with an increase in the thickness of the TiN layer from 125 to 300 nm and an increase in the perfection of the texture with the (111) plane parallel to the growth surface, the macrostresses (i.e., the macrovolume-correlated change in the interplanar spacing in crystal lattices) slightly increase. At the same time, they reach a value of about -7 GPa, which is apparently the limiting value for elastic deformation by compression of the crystal lattice of vacuum-arc TiN coatings.

With a further increase in the thickness of the TiN layer, the values of compressive macrostresses change little with increasing texture perfection.

From results of measuring the mechanical characteristics (hardness H and plasticity index H/E^*) of coatings by nanoindentation can be seen that the highest hardness, corresponding to superhard materials, is possessed by coatings obtained in two modes: 1 – deposition time $\tau = 30$ s, residual gas pressure $2.7 \cdot 10^{-3}$ Pa; 2 – $\tau = 300$ s, nitrogen atmosphere pressure $6.7 \cdot 10^{-1}$ Pa. In this case, an increase in U_p , accompanied by an increase in the average energy and smearing of the interlayer boundaries as a result of the action of the radiation factor, leads to a slight decrease in hardness. The plasticity index also changes in a similar way.

It should be noted that, at the beginning of the discussion of the structural state of coatings as can be seen from Figure 2 columnar (fibrous) microstructure of vacuum-arc condensate growth is formed in a single-layer coating. Moreover, a pronounced unidirectional columnarity appears starting from a distance of 100–200 nm from the substrate, below which the strict orientation is violated (light area near the substrate in Figure 2). Similar columnarity also appears in relatively thick TiN layers of a multilayer coating (Figure 4 a). At the same time, pronounced delamination in multilayer coatings with both relatively thick TiN layers (about 600 nm,

Figure 4 a) and thin layers (about 125 nm, Figure 4 b) attracts attention. The reason for such delamination can be high stresses in the layers, leading to partial plastic flow at their interface.

This effect can also be caused by different structural states of the lower and upper parts of the layer in the period of the multilayer system.

From Figure 5 shows that the basis of the diffraction spectrum is the reflections from the TiN phase. Applying a bias potential leads to a change in the predominant orientation of crystallites from the [100] axis perpendicular to the growth surface at a low bias potential U_p to [111] at a high potential. Thus, the observed change in the structure in TiN layers with a thickness of 300 nm with an increase in U_p is similar to the observed structural changes in single-layer TiN coatings with a thickness of 7-8 μm [10].

The study of the elastic stress-strain state of multilayer coatings, carried out by the method of X-ray tensiometry (" $a\text{-sin}2\psi$ "-method), showed that an increase in the bias potential from "floating" to -70 V leads to an increase in compressive stresses in the TiN phase from -3.1 GPa at a "floating" potential to -6.6 GPa at $U_p = -70$ V. In this case, the development of high compressive strain in the crystal lattice causes a decrease in the average crystallite size from 19 nm to 11.8 nm. Apparently, the lattice deformation of 2.04–2.10 %, corresponding to compression stresses of $(-6.6 \dots -6.8)$ GPa, is the limit for the TiN phase obtained in our case, since a further increase in U_p to -200 V does not lead to a significant increase in the elastic stress-strain state. The consequence of such a high-energy effect is the improvement of the texture [111] with a simultaneous increase in the average crystallite size (from 11.8 nm to 17 nm) in the direction of incidence of film-forming particles and a decrease in the lattice period.

Probably, the main reason for the formation of an elastic stress-strain state of compression, starting from small layer thicknesses, is, in this case, implantation processes, which are accompanied both in thick coatings and in relatively thin layers (300 nm) by an increase in the crystal lattice period.

This is due to the fact that the high ion flux density characteristic of the vacuum-arc method determines, upon implantation of ions into near-surface layers, an increase in the lattice period and the formation of compressive stresses in the coating bonded to the substrate.

At a high negative bias potential ($U_p > -70$ V), the secondary sputtering of light atoms (to which nitrogen atoms can be attributed in the TiN system)

determines a decrease in the lattice period with a relatively small change in the compressive stress state, the development of which is determined by an excess of atoms in the intercrystallite region.

Thus, the nonmonotonic dependence of the grating period in an unstressed section on U_p (Figure 6 b) can be explained mainly by implantation processes ("in situ" implantation into the subsurface layers of a growing coating to a depth of up to 1 nm) at low values of U_p and relative depletion of the coating with light nitrogen atoms as a result of their sputtering from the growth surface at a high (-70V – 200 V) bias potential.

Vacuum-arc coatings based on TiN obtained according to different deposition technological parameters. An analysis of the effect of constant shear potential (U_p) and pressure on the structure, elastically stressed-deformed state and mechanical properties of coatings based on titanium nitride was carried out. Obtained regularities of changes in phase composition, structural stress state, hardness depending on the value of the shear potential.

5. Multilayer coatings TiN/MoN

The dependence of the phase composition on the preparation conditions was analyzed in most detail for titanium and molybdenum nitrides. Moreover, in the latter case, due to the high sensitivity of the phase composition to small changes in characteristics, the regularities obtained as a result of such a study are of the greatest interest. In [11–13], it was shown that an increase in nitrogen pressure leads to a phase transformation in the coating from bcc cubic Mo to hexagonal δ -MoN, through the formation of phases with a cubic (NaCl type) lattice Mo_2N and MoN: $\text{Mo} \rightarrow \gamma\text{-Mo}_2\text{N} \rightarrow \text{MoN} \rightarrow \delta\text{-MoN}$. The resulting phases have a different crystal lattice, which affects the properties of the coating [14]. The most significant factors that determine the phase composition during reactive vacuum arc sputtering are the energy of particles and the mobility of film-forming atoms on the surface, which determines the efficiency of the phase formation reaction and, in particular, affects the stoichiometry of the resulting phases.

Therefore, the next stage of the research was to establish the influence of deposition parameters on the features of the formation of multilayer coatings TiN/MoN.

X-ray fluorescence analysis of the obtained coatings showed that the mass composition of Ti and Mo atoms entering the coating is in the range of

(51...56) wt.% Mo / (49...44) wt.% Ti. This corresponds to the Ti/Mo atomic ratio for samples with a small and medium layer thickness of 2-10 nm Ti/Mo \approx 60/40, and for a long layer deposition time – 20 s (layer thickness \approx 20 nm), this ratio shifts to Ti/Mo \approx 70/30.

In Table 2 a list of the investigated samples, their number and initial phase-structural and stress states based on the generalized data of the X-ray structural investigation.

Table 2

**Technological parameters of obtaining coatings,
their phase composition and structural state.**

$p_N = 6.7 \cdot 10^{-1}$ Pa, $U_i = 2000$ V, $f = 7$ kHz, $\tau = 10$ μ s

Sample	U_p , V	Deposition time, s	Correlation TiN/Mo ₂ N, wt.%	Texture (hkl)	σ_{TiN} (σ_{Mo_2N}), GPa	a_0 , nm
L1	-230	3	90/10	(111)	-3,9	0.42618
L2	-230	10	60/40	(111)	-6,9	0.42378
L3	-230	20	80/20	(111)	-2,63	0.42517
L4	-40	3	TiN -100	(200)	-1,5	0.4248
L5	-40	10	60/40	(200)	-5,7 (-3,9)	0.4242 γ -Mo ₂ N-0.4169
L6	-40	20	80/20	(200)	-13	0.4251

It is convenient to consider the structural state of the obtained coatings by grouping them depending on the thickness of the layers into three different series.

The first series of samples: layer thickness 2 nm.

For this series at a substrate potential of -40V, the X-ray phase analysis shows the content of only one phase with a cubic fcc lattice (structural type NaCl) (Figure 8), which is typical for TiN at a low temperature.

At the same time, the alternation of metal Ti and Mo vaporizers during spraying in a nitrogen environment should lead to layer-by-layer formation of TiN and Mo₂N with a thickness ratio close to the atomic ratio of metal atoms, which according to elemental analysis corresponds to a Ti/Mo ratio equal to 60/40. The absence of the interphase boundary that appears in this case indicates the epitaxial growth of thin layers in this case, the lattice period of which is determined by stronger bonds in the titanium nitride

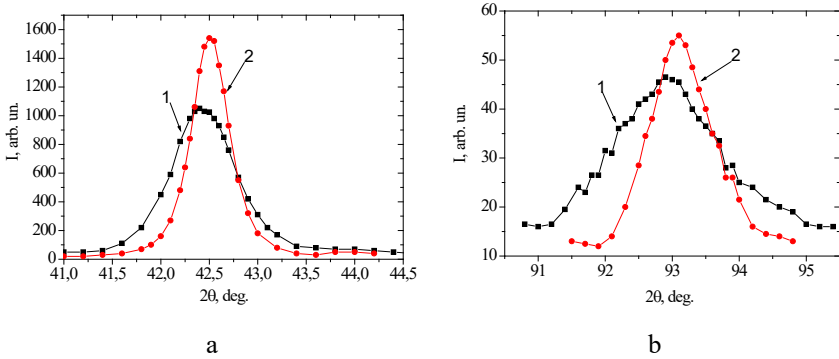


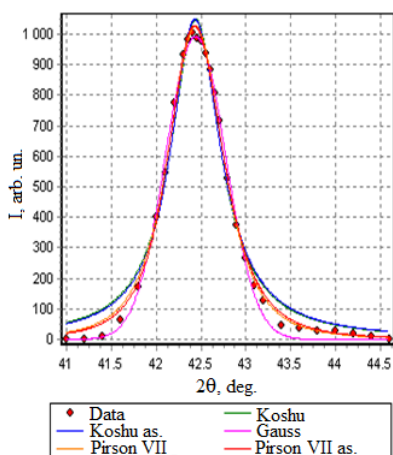
Figure 8. Comparative spectra of diffraction peaks for two orders of reflection from the texture plane (200) (a) and (400) (b) before (1) and after (2) annealing. (Sample L4)

layer. The period of the Mo_2N cubic lattice is 0.419 nm, that is, smaller than that of TiN, which contributes to the relaxation of compressive stresses in the epitaxial growth of the TiN layers and is accompanied by a decrease in the period in the unstressed section to 0.4248 nm (sample L4).

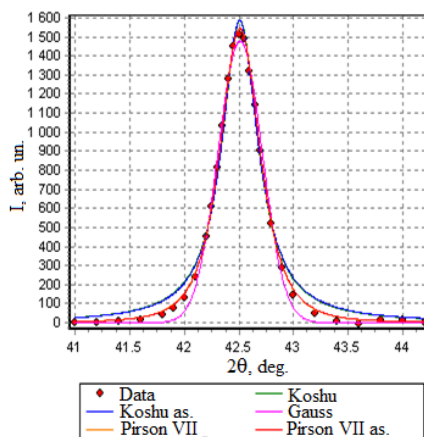
At the same time, in the case of formation as separate layers, Mo_2N layers with a cubic lattice, and accordingly, the formation of an interphase boundary leads to an increase in the voltage in the TiN phase and an increase in the period in the unstressed intersection. The selection of the Gaus function as the main one for approximation was based on the analysis of the profile shape with the full spectrum of possible approximating functions (Figure 9).

At a substrate potential of -230 V, X-ray phase analysis shows the formation of a two-phase material with the same type of crystal lattice (fcc type NaCl) TiN and high-temperature $\gamma\text{-Mo}_2\text{N}$ phases with a TiN/ Mo_2N phase ratio equal to 90/10. The reason for the appearance of the two-phase state in this case is the intense ion bombardment, which contributes to the grinding of grains and the formation of interphase boundaries. At the same time, the formation of separate layers of Mo_2N with a cubic lattice and, accordingly, the formation of an interphase boundary leads to an increase in the stress in the TiN phase and an increase in the period in the unstressed intersection (sample L1).

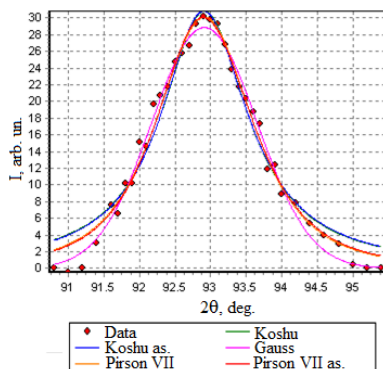
As the potential of the substrate increases, the texture of the molded coating changes from the texture with the [100] to [111] axis, which is accompanied by an increase in hardness. Based on the isostructures of the cubic component phases with their complete epitaxy, when there is no pro-



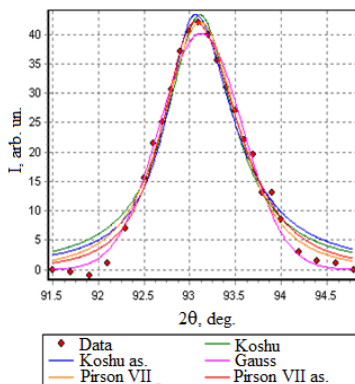
Sample L4 (200)



Sample L4 (200) annealing



Sample L4 (400)



Sample L4 (400) annealing

Figure 9. Using different approximating functions to describe the obtained diffraction profiles

nounced interphase boundary, and accordingly, the diffraction spectra show a spectrum characteristic of a single-phase state (see Figure 8), the material strengthens relatively weakly, which is manifested in the low hardness of such coatings and their fall during annealing (Sample L4).

The second series of samples: the thickness of the layer is about 10 nm.

For the second series of samples with a greater thickness of the component layers, the formation of a two-phase structural state with an average content of TiN and γ -Mo₂N cubic phases as 60 vol.%-40 vol.%, which is close to the results of X-ray fluorescence elemental analysis of atomic % components, is characteristic already during the deposition process metal atoms.

The appearance of a significant specific volume of interphase boundaries due to the high content of the second γ -Mo₂N phase (Figure 10) is accompanied by the development of high compressive stress in titanium nitride (Table 2). An exception is the sample obtained at a substrate potential of -230 V with a shorter lattice period, the reason for which may be the lack of nitrogen atoms in the coating compared to the stoichiometric composition, which can be judged by the decrease in the lattice period of

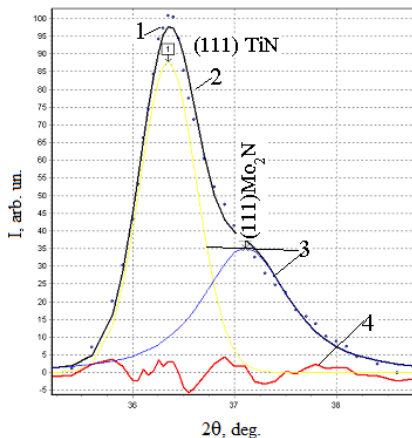


Figure 10. Distribution of diffraction spectra into components of spears from the two phases (111) TiN and (111) γ -Mo₂N (sample L2):
 1 – points of the initial data array, 2 – approximating curve,
 3 – selected spears, 4 – curve of misalignment

titanium nitride, which is 0.42378 nm (table the value for the stoichiometric composition is 0.42417 nm).

It is noteworthy that only the γ -Mo₂N phase is present in the molybdenum nitride layers and the β -Mo₂N phase is absent, although both of these phases are present in vacuum-arc monolayer coatings. This can be explained by the two-stage formation of the phase composition of the TiN/Mo₂N multilayer system, when at the initial moment of Mo₂N growth, the atomic sequence of the basic lattice of TiN is layered in such a way that determines the nucleation. Thus, there is a stabilization of the cubic modification of γ -Mo₂N during the growth of the molybdenum nitride layer, which, having reached a relatively large thickness due to the effect of structural macrostresses, is accompanied by a reset of the macrodeformation and the formation of an interphase boundary.

The third series of samples: the thickness of the layer is 20 nm.

Samples with the thickest layers of TiN, alternating with Mo₂N layers, obtained by the modes of the 3rd series, are also two-phase (Figure 11). however, the volume content of the molybdenum nitride phase before annealing (20%, Table 2, Figure 11 a) is somewhat lower compared to the data expected from the results of elemental X-ray fluorescence analysis (30%). At the same time, after annealing, the volume content of sufficient phases exactly corresponds to that expected according to elemental analysis data of 70% TiN – 30% Mo₂N.

This fact can be explained by the appearance for coatings of the 3rd series of a more blurred interphase boundary, which increases the contribution to the diffraction effect of the phase with a large volume content, in this case the titanium nitride phase. From behind the blurred boundary in this case, the correspondence of the phase composition to the elemental composition is manifested after annealing, when the specific contribution of the boundaries is significantly reduced, as a result of the transition of the material of the border region from the amorphous to the crystalline state.

6. Conclusions

The scientific problem was solved in the work, the reasons for the observed changes are established, which are based on the mechanism of formation of surface layers of vacuum-arc coatings under the condition of

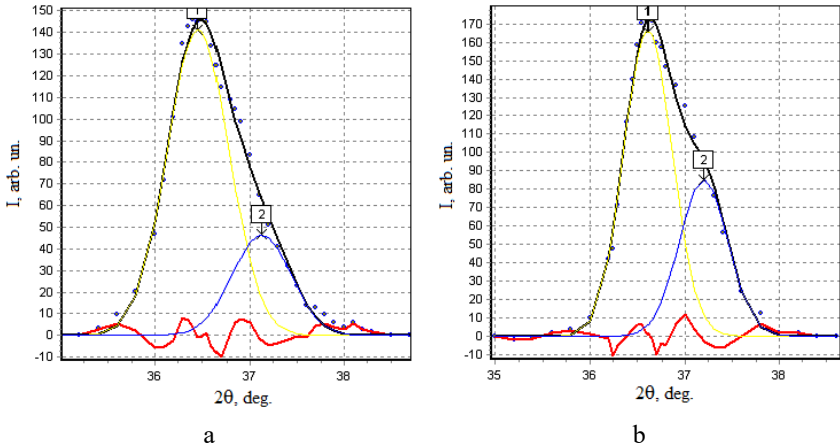


Figure 11. Distribution of diffraction spectra into component peaks from two phases (111) TiN and (111) γ -Mo₂N (sample L3) before annealing (a) and after annealing (b): 1 – points of the initial data array, 2 – approximating curve, 3 – selected spears, 4 – curve of misalignment

implantation processes stimulated by applying a negative potential to the substrate. It is established that:

1. In multilayer nanostructured TiN/Ti coatings, a texture develops in titanium nitride layers 300 nm thick or more when a bias potential is applied [11]. The degree of texture perfection increases with increasing layer thickness, which indicates the growth character of its nucleation, stimulated by radiation bombardment during the deposition of vacuum-arc coatings.

2. Thicknesses of Ti layers greater than 30 nm are sufficient for the development of the stress-strain state in TiN layers to proceed without their significant relaxation. A similar effect is also manifested with thicker titanium layers: 125 and 250 nm.

3. With an increase in the bias potential, the macrostresses of compression in the layers of titanium nitride TiN increase. Moreover, the maximum value of compression macrostresses is already achieved at relatively low values of $U_p = -40 \text{ V} \div -70 \text{ V}$. At higher U_p , while maintaining a practically constant value of compressive macrostresses of about -6.8 GPa, there is

an increase in texture perfection (which leads to an increase in the relative intensity of texture peaks) and depletion in light atoms (which causes a decrease in the period in the unstressed section).

4. The special features of the molding of bagato-ball covers have been installed TiN/MoN. With a small volume of balls of ≈ 2 nm, a possible epitaxial growth of isostructural cubic modifications of titanium nitride and molybdenum nitride without the adoption of a two-phase mill.

5. With a larger volume of balls 10... 20 nm, a two-phase material is molded, where the other phase is high-temperature molybdenum nitride γ -Mo₂N with a cubic lattice.

6. Increasing the volume of balls with a diameter of 2 to 20 nm increases the thermal stability of the mechanical powers of such coatings up to high-temperature (800°C) temperatures. For the shortest interval of the community of the balls of 2... 20 nm, the high-temperature temperature should not be changed until the phase structure of the coatings is changed, flooding the molybdenum nitride in the metastable γ -Mo₂N steel with a cubic lattice.

7. The reason for the stimulation during precipitation and stabilization when γ -Mo₂N is ignited is the influx of another warehouse rich ball system – titanium nitride (TiN), which is a high energy bond between metal and nitrogen atoms.

References:

1. Veprek S., Veprek-Heijman M.G.J., Karvankova P., Prochazka J. (2005) Different approaches to superhard coatings and nanocomposites. *Thin Solid Films*, vol. 476, iss. 1, pp. 1–29.
2. Sobol' O.V. (2007) Process nanostrukturhnogo uporyadocheniya v kondensatah sistemy W–Ti–B [The process of nanostructural ordering in condensates W–Ti–B systems]. *Solid state physics*, vol. 49, no. 6, pp. 1104–1110. (in Russian)
3. Pinchuk N., Sobol' O. (2020) Effects of high-voltage potential bias in pulsed form on the structure and mechanical characteristics of multilayer and multielement coatings obtained by vacuum arc evaporation. *Grabchenko's international conference: Advanced manufacturing processes (InterPartner–2019)*. (Odessa, 10-13 September 2019), Springer Science and Business Media Deutschland GmbH, pp. 451–460.
4. Genzel C., Reinmers W. (1998) A Study of X-ray residual-stress gradient analysis in thin-layers with strong filer texture. *Phys. Stat. Solidi: A-Applied Research*, vol. 166, no. 2, pp. 751–762.
5. Gargaud P., Labat S., Thomas O. (1998) Limits of validity of the crystal-lite group method in stress determination of thin film structures. *Thin Solid Films*, vol. 319, pp. 9–15.

6. Sobol' O.V., Andreev A.A., Stolbovoy V.A. and Filchikov V.E. (2012) Structural-phase and stresses state of vacuum-arc-deposited nanostructural Mo-N coatings controlled by substrate bias during deposition. *Technical Physics Letters*, vol 38, no, 2, pp. 168–171.
7. Helmersson H., Todorova S., Barnett S.A., Sundgren J.E., Markert L.C. and Greene J.E. (1987) Growth of single-crystal TiN/VN strained-layer superlattices with extremely high mechanical hardness. *Appl. Phys.*, vol. 62, no. 2, pp. 481–484.
8. Barnett S.A., Francombe M., Vossen J.A. (1993) Physics of thin films. *Mechanic and Dielectric Properties*, edited by MH Francombe and JL Vossen (Academic, Boston, 1993). T. 17.
9. Fromm E., Gebhard E. (1980) Gazy i uglerod v metallah [Gases and carbon in metals]. M.: Metallurgiya, 593 p. (in Russian)
10. Sobol' O., Andreev A. and etc. (2011) Physical characteristics, structure and stress state of vacuum-arc TiN coating, deposition on the substrate when applying high-voltage pulse during the deposition. *VANT*, no. 4(98), pp. 174–177.
11. Urgan M., Eryilmaz O.L., Cakir A.F., Kayali E.S., Nilufer B., Isik Y. (1997) Characterization of molybdenum nitride coatings produced by arc-PVD technique. *Surf. Coat. Tech.*, vol. 94-95, pp. 501–506.
12. Maoujoud M., Binst L., Delcambe P., Offergeld-Jardinier M., Bouillon F. (1992) Deposition parameter effects on the composition and the crystalline state of reactively sputtered molybdenum nitride. *Surf. Coat. Tech.*, vol. 52, no. 2, pp. 179–185.
13. Perry A.J., Baouchi A.W., Petersen J.H., Pozder S.D. (1992) Crystal structure of molybdenum nitride films made by reactive cathodic arc evaporation. *Surf. Coat. Tech.*, vol. 54-55, part 1, pp. 261–265.
14. Kazmanli M.K., Urgan M., Cakir A.F. (2003) Effect of nitrogen pressure, bias voltage and substrate temperature on the phase structure of Mo–N coatings produced by cathodic arc PVD. *Surf. Coat. Tech.*, vol. 167, no. 1, pp. 77–82.